

## EFFECTS OF PROTON IRRADIATION ON THE SPECTRAL PERFORMANCE OF PHOTOVOLTAIC CELLS BASED ON CdS/CdTe THIN FILMS

L. ION<sup>a</sup>, I. ENCULESCU<sup>b</sup>, S. IFTIMIE<sup>a</sup>, V. GHENESCU<sup>c</sup>, C. TAZLAOANU<sup>a</sup>,  
C. BESLEAGA<sup>a</sup>, T. L. MITRAN<sup>a</sup>, V. A. ANTOHE<sup>a</sup>, M. M. GUGIU<sup>d</sup>,  
S. ANTOHE<sup>a</sup>

<sup>a</sup>*Department of Solid State Physics, University of Bucharest, 077125, Magurele-Ilfov, Atomistilor 405, Romania*

<sup>b</sup>*National Institute for Materials Physics, 077125, Magurele-Ilfov, Atomistilor 105b, Romania*

<sup>c</sup>*Institute of Space Sciences, 409 Atomistilor, 077125, Magurele-Ilfov, Romania*

<sup>d</sup>*National Institute of Physics and Nuclear Engineering - IFIN HH, 077125, Magurele-Ilfov, Atomistilor 407, Romania*

Due to their physical and chemical properties (such as suitable band gaps, large absorption coefficients and good chemical stability) CdTe thin films are interesting for electronic and optoelectronic devices, including particularly photovoltaic cells for space technology. For that specific application, it is of prime importance to study in this type of materials the influence of ionizing radiations on their physical (structural, electrical and optical) properties. In this paper, the photovoltaic cells based on CdS/CdTe thin films, produced by thermal vacuum sublimation, were irradiated with 3 MeV protons at room temperature. The effects of irradiation were studied by investigating the changes in the electrical and optical properties of the cells. It was found that proton irradiation in the above mentioned conditions results mainly in the introduction of defects at the CdS/CdTe interface. A discussion about the possible origin of those defects is given.

(Received August 20, 2010); accepted August 31, 2010)

*Keywords:* Solar cells, Cadmium Telluride, Thin Films, Proton Irradiation

### 1. Introduction

Thin film CdS/CdTe photovoltaic cells are among the best candidates for producing low cost and high efficient heterojunction photovoltaic devices [1-5]. They were produced in both superstrate and substrate configurations, using several types of techniques [6]. In addition, the good stability of CdTe based solar cells against proton irradiation was demonstrated [7], which recommends them for use in space technology.

Results of studies on the effects of electron and proton irradiation on physical properties of individual layers (i.e. CdS, CdTe and CdSe thin films) were reported elsewhere [8-16]. In the case of proton irradiation, it was found that 3 MeV accelerated proton irradiation, at relatively high fluencies (up to  $10^{14}$  cm<sup>-2</sup>) results mainly in the introduction of point-like defects, acting as traps for free carriers. But, relatively few works were devoted to study the effect of ionizing irradiation on the performance of photovoltaic cells based on these materials [17]. In this paper we report the results we have obtained on the effects of proton irradiation (3 MeV energy and  $3 \times 10^{13}$  protons/cm<sup>2</sup> fluency) on the main parameters of CdS/CdTe thin film photovoltaic cells. The aim of this study was to investigate the changes induced in the spectral dependence of the photovoltaic response of the cells by the irradiation with protons in the above-mentioned conditions.

## 2. Experimental details

CdS/CdTe photovoltaic cells were developed on ITO coated optical substrates, by thermal vacuum evaporation of CdS, respectively CdTe powder, in superstrate configuration. First, the CdS layer was sublimated at a pressure of  $3.2 \times 10^{-4}$  mbar from a quartz container heated to 740°C, the substrate temperature being maintained at 250°C. To prevent the sputtering of the powder during evaporation, the container was covered with a quartz-wool plug. After deposition, to improve the structural quality of the films, they were thermally treated in vacuum at 350°C for 15 minutes. Next, the CdTe layer was sublimated at 600°C, with the substrate at 250°C and the heterostructure was thermally treated in vacuum at 350°C for 18 minutes. A back contact was evaporated on top of the CdTe layer, to complete the cell structure, consisting of 50 nm copper layer and 100 nm gold layer. After the Cu electrode deposition an annealing treatment in vacuum at 200°C for 15 minutes was applied.

The cells were subjected to irradiation from the backside with protons supplied by an accelerator, the proton beam being directed along the normal to the surface of the samples. Irradiation was carried out in an evacuated chamber, at ambient temperature, with 3 MeV protons to a fluency of  $3 \times 10^{13}$  protons/cm<sup>2</sup>. During irradiation the thermal effect was negligible.

The surface morphology of CdS and CdTe layers was analyzed by atomic force microscopy (AFM) and scanning electron microscopy (SEM). Their crystalline structure was studied by X-ray diffraction (XRD), using a Brucker Discovery D8 diffractometer.

Electrical characterizations in dark condition and under illumination were performed by using a Keithley 2400 SourceMeter, controlled by a computer, the light source was either an incandescence lamp or a Newport-Oriel 150 solar simulator. In the later case, all characterizations were performed in A.M. 1.5 conditions. For action spectra and external quantum efficiency (EQE) measurements, an experimental setup containing a Newport Oriel monochromator, controlled by a computer, was used. Optical properties of the CdS and CdTe films were characterized by performing transmittance and absorptions measurements. The data were recorded at room temperature, with a Perkin-Elmer Lambda 35 spectrometer.

## 3. Results and discussion

### 3.1 Crystalline Structure

Structural analysis of the CdS films revealed that they consist of a well formed würtzite type phase, with (002) preferred orientation (fig. 1a). The XRD pattern of the CdTe films, grown in the above mentioned conditions, shows peaks related to the face-centered cubic phase of zinblende type (fig. 1b). CdTe layer show a good (111) texture, corresponding to the fast growth direction of this compound [18] and also related to the CdS substrate orientation.

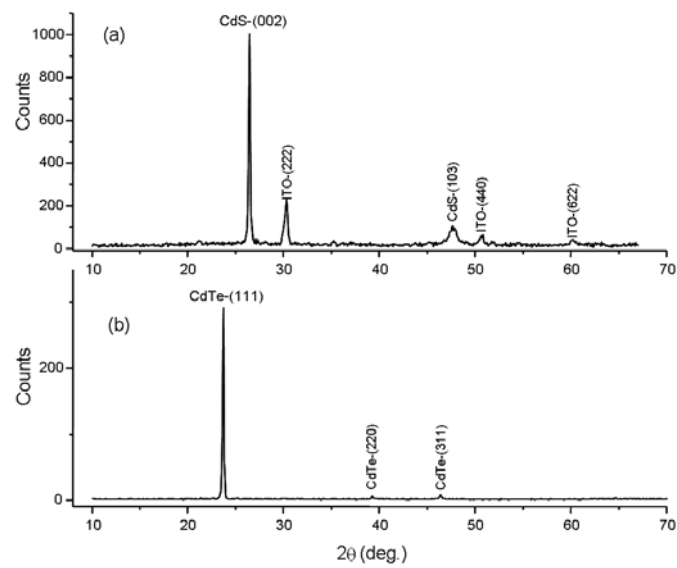


Fig. 1. XRD pattern of the CdS layer (a) and of the CdTe layer of the cell (b)

### 3.2 Morphology

Cross-section SEM micrograph of one of the cells and AFM scans are shown in figures 2a, 2b and 2c. Both SEM and AFM images show that the films are made out of dense and well faceted crystallites, with linear transversal dimensions larger than 100 nm.

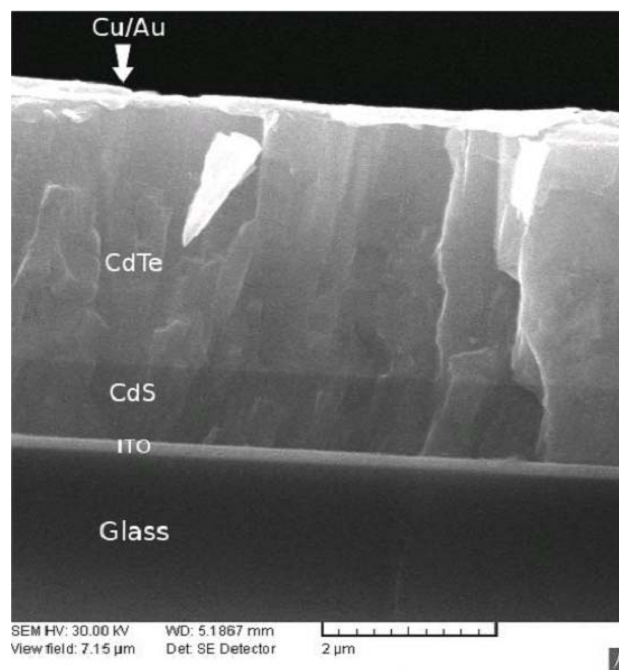


Fig. 2a. Cross-section SEM micrograph of the CdS/CdTe cell

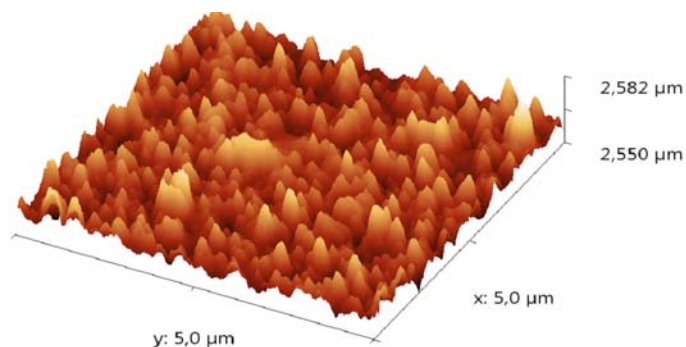


Fig. 2b. AFM image of the surface of the CdS layer

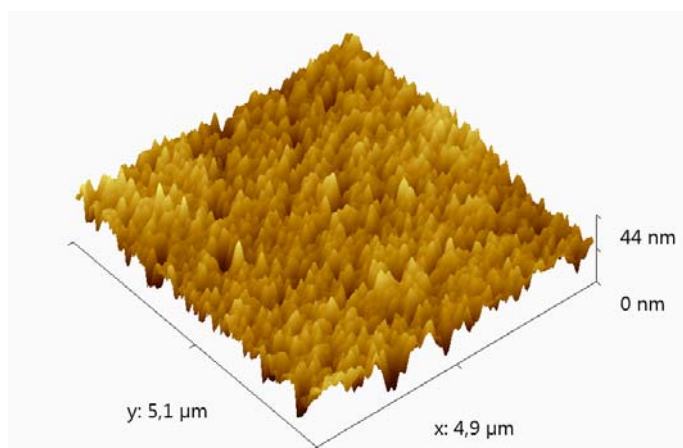


Fig. 2c. AFM image of the surface of the CdTe layer

Cross-section elemental mapping of the CdS/CdTe heterojunction, obtained by Energy Dispersive X-ray (EDX) analysis (Fig. 3) suggest that inter-diffusion of S and Te atoms has occurred at the interface, possibly with the formation of a  $\text{CdTe}_{1-x}\text{S}_x$  compound. This process was induced either during CdTe deposition or the subsequent vacuum annealing treatment of the cell.

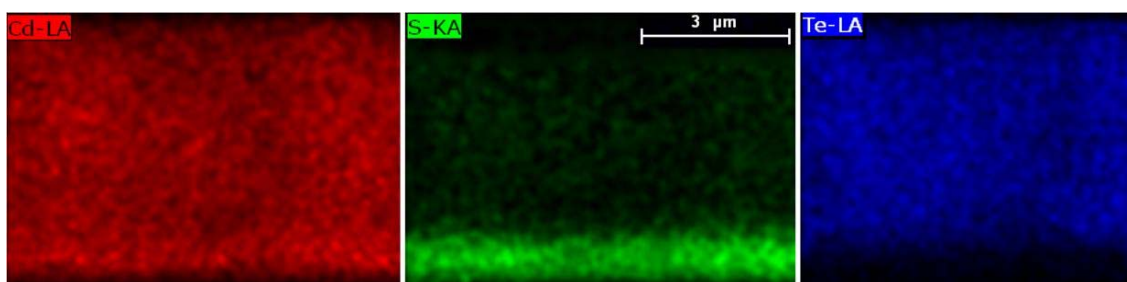


Fig. 3. EDX mapping of the CdS/CdTe junction.

### 3.3 Current-Voltage characteristics in the dark

The current-voltage (I-V) characteristics of an ITO/CdS/CdTe/Cu/Au cells measured in dark, before irradiation, at room temperature, in both forward and reverse bias conditions, are shown in figure 4. As expected, the forward bias conditions correspond to positive voltage on the gold electrode with respect to the ITO front contact electrode. A thorough analysis of the dark I-V characteristics of the cell, starting from the modified Shockley equation [19], allows for a characterization of CdS/CdTe interface, responsible for both electric and photovoltaic behavior of the cell.

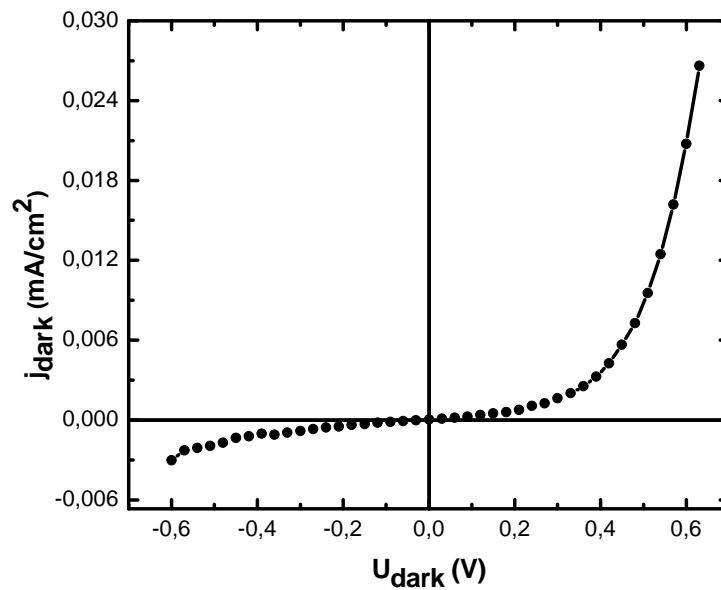


Fig. 4. *I-V characteristics of ITO/CdS/CdTe/Cu/Au cell in the dark*

The modified Shockley equation is given by:

$$I = I_o \left\{ \exp[\beta(V - IR_s)] - 1 \right\} + \frac{V - IR_s}{R_{sh}} \quad (1)$$

where:  $I_o$  is the reverse saturation current,  $R_s$  – the series resistance and  $R_{sh}$  – the shunt resistance. Here  $\beta = q/nkT$ , where  $q$  is the electronic charge,  $n$  – the diode quality factor,  $k$  – the Boltzmann constant, and  $T$  – the absolute temperature. The differential resistance of the cell is given by:

$$R_o = \frac{dV}{dI} = R_s + \frac{1}{\left\{ \beta I_o \exp[\beta(V - IR_s)] + \frac{1}{R_{sh}} \right\}} \quad (2)$$

At high voltages, in forward bias, eq. (1) becomes  $I = I_o \exp[\beta(V - IR_s)]$  and then Eq. (2) simplifies to:

$$R_o \cong R_s + \frac{1}{\beta I} \quad (3)$$

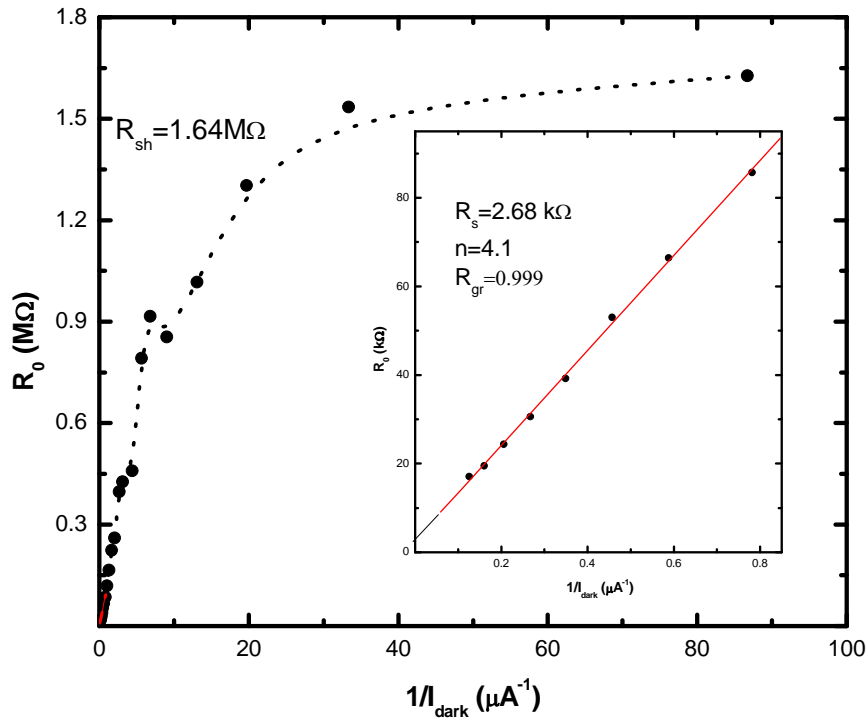


Fig. 5. Dependence of the differential resistance of ITO/CdS/CdTe/Cu/Au cell on the reciprocal of the current at forward bias

Thus, in the range of high voltages of  $R_0$  vs.  $1/I_{\text{dark}}$  plot, shown in figure 5, the values for  $R_s$  and  $n$  parameters can be extracted. At low voltages, where the current flowing through  $R_{sh}$  becomes important, eq. (2) becomes  $R_o \cong R_s + R_{sh}$ . Since  $R_s \ll R_{sh}$ , it follows that  $R_o$  is essentially  $R_{sh}$  at low voltages. The values of  $R_s$  and  $R_{sh}$  are:  $R_s = 2.68 \text{ k}\Omega$  and  $R_{sh} = 1.64 \text{ M}\Omega$ . Further on, in order to get more accurately the values of  $I_0$  and  $n$ , eq. (1) has been transformed as:

$$I - \frac{Y}{R_{sh}} = I_o [\exp(\beta Y)] \quad (4)$$

where:  $I - \frac{Y}{R_{sh}}$  is the current flowing through the barrier and  $Y = V - I R_s$ , the real voltage drop across it, respectively.

The plot of  $\ln\left(I - \frac{Y}{R_{sh}}\right)$  vs.  $Y$  is shown in figure 6. After removing the effects of series and shunt resistances, the linear part in the plot was extended considerably, increasing the accuracy in the determination of  $I_0$  and  $n$  values, respectively  $I_0 = 9.6 \times 10^{-9} \text{ A}$  and  $n = 3.46$ .

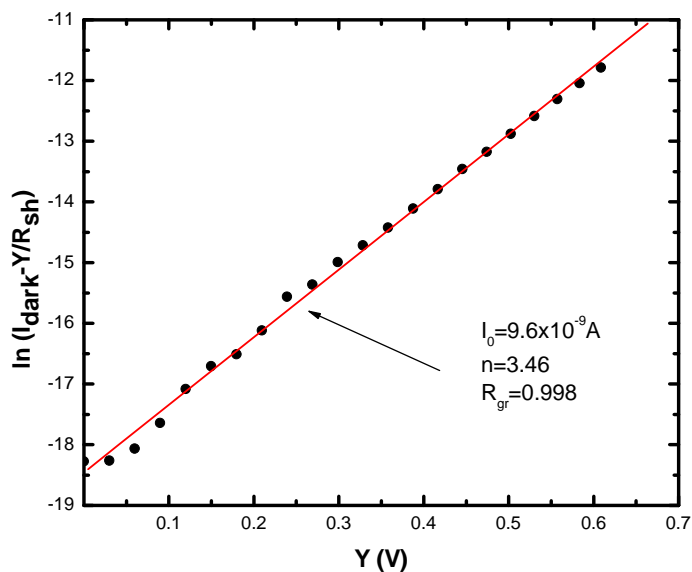


Fig. 6. The  $\ln(I - Y/R_{sh}) = f(Y)$  characteristics for ITO/CdS/CdTe/Cu/Au cell

### 3.4 Current-Voltage characteristics, at illumination in fourth quadrant

Typical I-V characteristics in the fourth quadrant, under AM1.5 conditions, measured before and after irradiation, are shown in figure 7.

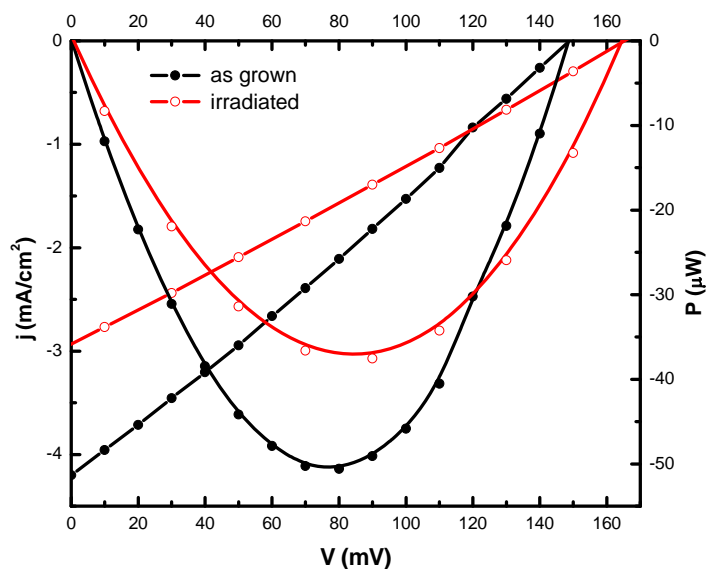


Fig. 7. I-V characteristics of the ITO/CdS/CdTe/Cu/Au device measured under AM 1.5 illuminations, before (open red circles) and after (filled black circles) irradiation

The main parameters of the photovoltaic cells, derived from I-V measurements before and after irradiation, are shown in table 1.

Table 1. I-V parameters of the cell before and after irradiation

Parameter	As grown	Irradiated
$V_{OC}$ (mV)	149	165
$I_{SC}$ (mA/cm <sup>2</sup> )	4.2	3.0
FF (%)	27.2	25.6

### 3.5 Spectral characterization

Figure 8 shows the spectral dependence of the normalized external quantum efficiency (EQE) recorded for one of the cells, both before and after irradiation with 3 MeV protons. From near-threshold absorption spectra, bandgap values of 1.48 eV and 2.32 eV were determined for CdTe (fig. 8, dashed line) and CdS (fig. 8, solid line) layers, respectively. Before irradiation, the spectral photovoltaic response of this cell fits well with the spectral dependence of the optical absorption coefficient of the CdTe layer, at photon energies greater than the band-gap (i.e., 1.48 eV), where EQE rises steeply. With the onset of the fundamental absorption in CdS, EQE drops rapidly, proving that the space-charge region of the heterostructure extends mainly in the CdTe layer. The group of three peaks that can be clearly seen at photon energies below the bandgap of CdTe, respectively at 1.16 eV, 1.26 eV and 1.35 eV correspond to electron transitions from defect (acceptor) bands to the conduction band of the host material. We infer that these defects are associated with the observed S and Te inter-diffusion at the CdS/CdTe interface.

It is worth mentioning that in CdTe, the singly ionized Cd vacancy  $V_{Cd}^-$  is an acceptor defect with a level located at 0.13 eV above the valence band maximum [20,21]; the observed peak at 1.35 eV could be associated to the electron transition from this level to the conduction band.

After irradiation, the fourth quadrant of I-V characteristics was not significantly changed, but the structure of the EQE spectrum is substantially altered: its background level increases in the whole investigated spectra range, the main feature now correspond to the above mentioned defects, while EQE values decrease significantly for photon energies in the range corresponding to absorption in CdTe, (i.e., 1.48 eV, 2.5 eV), and increase for photon energies in the range corresponding to fundamental absorption in CdS layer proving that the space-charge region is now more extended into CdS layer.

In order to get a more detailed image of the proton irradiation damage in our cell, the software package SRIM-2008 [22] was used in full collision cascade mode. Figure 9 shows the result of a Monte-Carlo simulation of protons spatial scattering distribution and the S and Te recoil atom distributions. At this proton energy most of these protons are transmitted, but a significant damage can be observed at the CdS/CdTe interface, where most of the vacancies are produced in CdTe layer and inter-diffusion of S and Te recoil atoms occurs (fig. 9b).

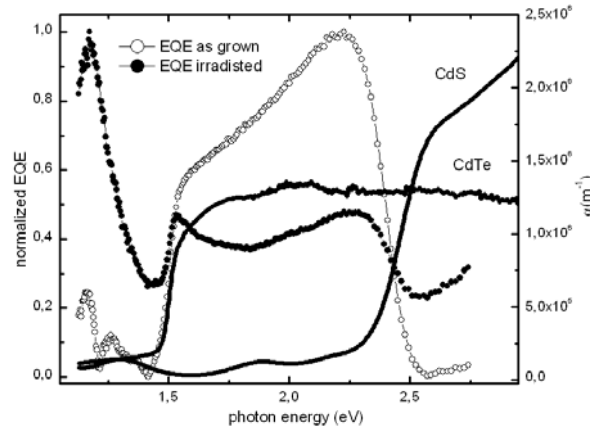


Fig. 8. Normalized EQE spectrum before (open circles) and after (filled circles) irradiation with 3 MeV protons and absorption spectra of constitutive CdTe (dashed line) and CdS (solid line) layers of the cell

We associate the observed increase of the EQE at photon energies below the optical threshold of CdTe with this effect. After irradiation the peak structure in this spectra range is washed out; only the peak at 1.16 eV was observed, with a shoulder at 1.26 eV.

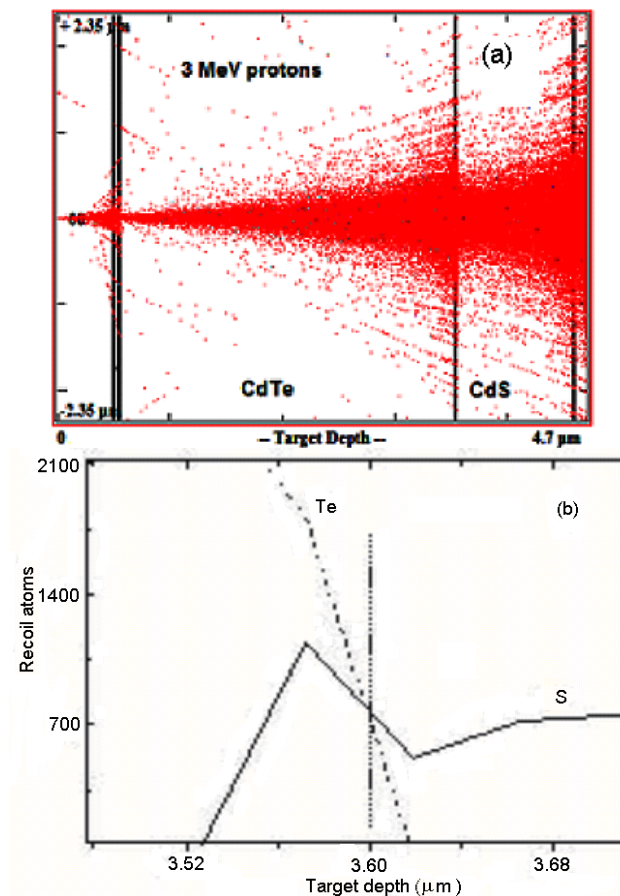


Fig. 9. Monte-Carlo simulation of 3 MeV proton scattering distribution (a) and S and Te recoil atoms distribution in CdS/CdTe cell (b)

EQE decreasing in the spectral range corresponding to photo-generation of free carriers in CdTe can be related to the decrease of their life time due to irradiation damage.

#### 4. Conclusions

The ITO/CdS/CdTe/Cu/Au photovoltaic cells were prepared and characterized, investigating the effect of proton irradiation on their performances. It was found that irradiation with 3 MeV protons at fluencies up to  $3 \times 10^{13}$  protons/cm<sup>2</sup> affect only slightly the main parameters (short-circuit current, open-circuit voltage, fill factor) and the overall performance of the cells.

At this energy, most of the incident protons are transmitted and significant radiation damage occurs mainly at CdS/CdTe interface. Important changes were detected in the spectral dependence of EQE, especially in the spectral range corresponding to incident photons with energies below the bandgap of the base absorber layer (CdTe). We infer that these changes are due to defects associated with inter-diffusion of S and Te recoil atoms.

### Acknowledgments

The National Authority for Scientific Research of Romania supported this work under Grant no. PN II 81-030/2007.

### References

- [1] M. A. Cousins, K. Durose, *Thin Solid Films* **361/362**, 253 (2000)
- [2] D. L. Baltzner, G. Agostinelli, M. Campo, A. Romeo, J. Beier, H. Zogg, A. N. Tiwari, *Thin Solid Films* **431/432**, 421 (2003)
- [3] J. Fritsche, T. Schulmeyer, A. Tiesen, A. Klein, W. Jaegermann, *Thin Solid Films*, **431/432**, 267 (2003)
- [4] G. G. Rusu, M. Rusu, E. K. Polychroniadis, C. Lioutas, *J. Optoelectron. Adv. Mater.* **7**(4), 1957 (2005)
- [5] I. Salaoru, P. A. Buffat, D. Laub, A. Amariei, N. Apetroaei, M. Rusu, *J. Optoelectron. Adv. Mater.* **8**(3) 936 (2006)
- [6] A. Romeo, M. Terheggen, D. Abou-Ras, D.L. Bätzner, F.-J. Haug, M. Kälin, D. Rudmann, A. N. Tiwari, *Prog. Photovolt.: Res. Appl.* **12**, 93 (2004).
- [7] A. Romeo, D.L. Bätzner, H. Zogg, A.N. Tiwari, *Mater. Res. Soc. Symp. Proc.* **668**, H3.3.1 (2001).
- [8] L. Ion, V.A. Antohe, M. Ghenescu, O. Ghenescu, R. Bazavan, M. Danila, M.M. Gugiu, S. Antohe, *Mater. Res. Soc. Symp. Proc.* **1012**, 343 (2007).
- [9] S. Antohe, L. Ion, V.A. Antohe, M. Ghenescu, H. Alexandru, *J. Optoelectron. Adv. Mater.* **9**, 1382 (2007).
- [10] S. Antohe, V. Ruxandra and H. Alexandru, *Journal of Crystal Growth*, **237-239**, 1559 (2002).
- [11] L. Ion, S. Antohe, M. Popescu, F. Scarlat, F. Sava and Felicia Ionescu, *J. Optoelectron. Adv. Mater.* **6**(1), 113 (2004)
- [12] L. Ion, S. Antohe, *J. Appl. Phys.* **1**, 3513 (2005)
- [13] L. Ion, V. A. Antohe, S. Antohe, *J. Optoelectron. Adv. Mater.* **7**(4), 1847 (2005).
- [14] R. Bazavan, O. Ghenescu, M. Ghenescu, D. Crisan, A. Radu, L. Ion, S. Antohe, *J. Optoelectron. Adv. Mater.* **11**, 3048 (2008).
- [15] Veta Ghenescu, L. Ion, M. Ghenescu, M. Rusu, M. Gugiu, G. Velisa, Oana Porumb, S. Antohe, *Optoelectron. Adv. Mater.-Rapid Comm.* **3**(10), 1023 (2009).
- [16] L. Ion, V. Ghenescu, S. Iftimie, V. A. Antohe, A. Radu, M. Gugiu, G. Velisa, O. Porumb, S. Antohe, *Optoelectron. Adv. Mater.-Rapid Comm. (OAM-RC)* **4**(8), 1114 (2010).
- [17] D. L. Bätzner, A. Romeo, M. Dobeli, K. Weinert, H. zogg, A. N. Tiwari, 29<sup>th</sup> PVSC, New Orleans (2002)
- [18] J. Luschitz, B. Siebchen, J. Schaffner, K. Lakus-Wollny, G. Haindl, A. Klein, W. Jaegermann, *Thin Solid Films* **517**, 2125 (2009).
- [19] Antohe, S.; Ruxandra, V.; Tugulea, L.; Gheorghie, V.; Inascu, D.; *J. Phys. III France* **6**, 1133 (1996).
- [20] Su-Huai Wei and S.B. Zhang, *Phys. Rev. B* **66**, 155211 (2002)
- [21] F.H. Seymour, V. Kaydanov, T.R. Ohno, *Appl. Phys. Lett.* **87**, 153507 (2005)
- [22] J.F. Ziegler, J.P. Biersack, U. Littmark, *The stopping and range of ions in solids*, Pergamon Press, New York, 1985